Bull. Mater. Sci., Vol. 15, No. 5, October 1992, pp. 411–420. © Printed in India.

Nanocomposites

D CHAKRAVORTY
Indian Association for the Cultivation of Science, Jadavpur, Calcutta 700032, India

Abstract. Nanocrystalline metals having sizes of the order of a few nanometres dispersed in an oxide glass matrix have been discussed in this review. The various physical and chemical routes developed so far for synthesizing such materials have been described. The different physical properties, especially optical, electrical and magnetic behaviour of these nanocomposites have been delineated. The physical mechanisms which give rise to these characteristics are discussed.

Keyword. Nanocomposites.

1. Introduction

Nanocomposites consist of two or more phases, each having nanometre dimensions. A particular case is the dispersion of a phase having nanometre dimensions within a host matrix glass. A few of the examples where such a configuration has been exploited in practical applications are cermets (Abeles *et al* 1975), photosensitive, photochromic and polychromatic glasses (Armistead and Stookey 1965; Stookey *et al* 1978). Cermets are composites where nanometre sized metals are dispersed in an oxide (ceramic) matrix whereas photosensitive and photochromic action in glasses arise due to the precipitation of nanoscale metal clusters within them. Polychromatic glasses also have ultrafine metal particles but these are grown on some pyramid shaped crystallites of a suitable inorganic compound like NaF.

In recent years nanocrystalline materials have attracted considerable attention (Andres *et al* 1989). These are polycrystalline materials with a crystallite size of the order of a few nanometres. Interest in these systems has arisen because of novel physical properties expected in matter having such ultrafine dimensions. The behaviour of such nanoscale clusters will neither correspond to those of free atoms or molecules making up the particle nor to that of the bulk solid with an identical chemical composition. Considering the various methods developed so far for making these nanocrystalline solids it appears that the so-called grain boundary structure in them is drastically different from that of the crystalline core. The structure cannot be described as a disordered one (Birringer *et al* 1984). Also the volume fraction of this interfacial component in these materials is comparable to that of the crystals. It therefore appears that what we refer to as a nanocrystalline material is, strictly speaking, a nanocomposite. Depending on the route followed for the synthesis of nanoclusters of different species, the matrix phase could either have the same chemical composition as the nanophase or would comprise of different chemical species. In this article we briefly review the different synthetic routes developed so far for making nanocomposites and some of the interesting physical properties exhibited by them with special emphasis on their electrical, magnetic and optical behaviour.

2. Preparation

2.1 *Physical route*

Sputtering technique has been extensively used to make metal-ceramic composites with the metallic phase having nanometer dimensions (Abeles *et al* 1975). The procedure involves hitting the target surface by accelerating ions of elements like argon or krypton. In the case of cermet films the targets comprise the metal and the oxide respectively. Some of the systems prepared by this technique are Ni/SiO_2, Pt/SiO_2, Au/Al_2O_3 etc. The samples are produced in thin film form. Recently nanocomposites comprising germanium crystals with sizes varying from 5 to 12 nm in silica glass films have been made using conventional rf magnetron sputtering equipment (Hayashi *et al* 1990). A silica glass plate with a number of germanium polycrystalline chips on it has been used as the target in this method.

For synthesizing nanocrystalline materials especially metals the most common method used has been the inert-gas evaporation technique (Granqvist and Buhrman 1976). The latter consists of producing a vapour of the atoms from a source heated resistively in the presence of an inert gas like helium. Collision with the gas atoms brings about a lowering of temperature of the metal vapour which becomes highly supersaturated locally. Metal clusters then form on a liquid nitrogen cooled surface by a nucleation and growth mechanism. The particles are scraped off the surface and the powders are compacted under a pressure ranging from 1 to 5 GPa within the vacuum chamber (Birringer *et al* 1984). Oxides or other ceramic materials can be synthesized in their nanocrystalline forms by this method also by replacing the inert gas with a reactive one. A wide range of metals and some oxides have been prepared by this method and their properties delineated (for a review see Chakravorty and Giri 1992).

Recently nanocomposites of ultrafine iron particles in a metallic matrix have been synthesized by first making a metastable alloy of iron and copper (Fe_xCu_{1-x}) over the entire composition range by dc magnetron sputtering on to liquid nitrogen-cooled substrates. On subsequent heat treatment at elevated temperatures up to about 600°C recrystallization occurs with a transformation into separate phases of bcc Fe and fcc Cu. Iron particles of sizes varying from 15 to 60 nm have been prepared by this novel route (Childress *et al* 1990).

2.2 *Chemical route*

Sol–gel technique has emerged as a versatile method for synthesizing a wide range of materials (Chakravorty 1992). Nanocomposites have also been prepared by this method. Preparation of diphasic xerogels has been shown to lead to the formation of new hybrid ceramic-metal composites e.g. Ni/Al_2O_3, Cu/Al_2O_3, Cu/SiO_2, Cu/ZrO_2 etc (Roy and Roy 1984). The metal islands in such materials have diameters in the range of 5 to 50 nm. The method comprises preparation of a sol consisting of the oxide component and a solution containing the metallic salt, the latter being the metal phase precursor. The resulting xerogel has two noncrystalline oxide phases. This two-phase solid is then subjected to reduction treatment in a nitrogen and hydrogen gas mixture (95% N_2, 5% H_2) at temperatures ranging from 200 to 700°C. Some of the starting materials used are aluminium isopropoxide, zirconyl chloride and silicon tetraethoxide

respectively for the matrix phase and copper nitrate, nickel nitrate respectively for the metal phase.

A variant of the above method has been the use of suitable metal-organic compounds as metal precursors (Chatterjee and Chakravorty 1989). Some examples of the latter are nickel oxinate $Ni(C_9H_6ON)_2 \cdot 2H_2O$ and the pyridine complexes $[Me(C_5H_5N)_4](SCN)_2$ (where Me = Fe, Co or Mn). Glass metal nanocomposites have been synthesized from a precursor sol comprising the metal-organic compound and silicon tetraethoxide. The sol is allowed to gel. The latter is subsequently heat treated at temperatures ranging from 250 to 500°C for periods varying from a few minutes to one hour. The metal particle diameter is found to have values in the range 3 to 10 nm depending on the heat treatment schedule. Use of metal-organic compounds also obviates the need for hydrogen reduction treatment. The volume fraction of the metal phase in these composites has been only a few per cent. Detailed optical absorption studies have been carried out on these nanocomposites and will be discussed subsequently.

Glass metal composites with nanometre sized metal particles of types Fe/SiO_2, Ni/SiO_2 and Cu/SiO_2 respectively have also been synthesized in thick film form on a glass substrate by using a sol containing silicon tetraethoxide and a metallic salt in ethyl alcohol. For the different metallic species the salts used have been $FeCl_3$, $NiCl_2$ and $CuCl_2$ or $Cu(NO_3)_2$ respectively (Chatterjee and Chakravorty 1990). By varying the salt content in the sol it has been possible to generate both percolative as well as non-percolative configuration of the metal phase in the composite concerned. The electrical properties of these systems will be delineated in the following section.

Silver nanoparticles of size ranging from 4 to 12 nm have been grown at the glass-crystal interface of a suitably chosen glass-ceramic system (Roy and Chakravorty 1990). The precursor glass has the composition 55 SiO_2, 12 ZnO, 32·2 Li_2O, 0·8 P_2O_5 (mol%). After a ceramization treatment at 565°C for 1 h followed by 630°C for 3 h micron-sized crystallites of zinc orthosilicate (Zn_2SiO_4) and lithium phosphate ($Li_4P_2O_7$) are precipitated within the glass. The resultant glass-ceramic is subjected to a lithium silver exchange by immersing the sample in molten silver nitrate at 310°C for 8 hours. The ion exchanged specimen is then subjected to a reduction treatment in hydrogen at temperatures in the range 320 to 600°C for a duration extending from a few minutes to 1 hour. Electrical behaviour of the resultant metallic aggregates is discussed later.

3. Properties

3.1 *Optical*

Optical properties for ultrafine metal particles dispersed in a silicate glass matrix have been investigated by a number of authors (Doremus 1965; Kreibig 1974) because of the possibility of observing a quantum size effect. The latter has been predicted on the basis of the formation of discrete energy levels in small metal particles. However, plasma resonance absorption measurements on silver nanoparticles dispersed in an oxide glass down to a low temperature ($\sim$ 1·5 K) has given negative results (Kreibig 1974).

In figure 1 is shown the optical absorption characteristics for glasses containing different metallic species with nanometre dimensions in the wavelength region 0·2 to 2·0 m. The particle size in these systems is around 4 nm and the metal phases are nickel,

iron, manganese and cobalt respectively (Chatterjee and Chakravorty 1989). It is evident that the value of the optical absorption coefficient is dependent on the metal phase present. The optical absorption characteristics of these glass metal composites have been explained on the basis of Maxwell–Garnet model (Maxwell–Garnet 1904) which predicts the effective permittivity $\bar{\varepsilon}^{MG}$ given by

$$\frac{\bar{\varepsilon}^{MG} - \varepsilon_m}{\bar{\varepsilon}^{MG} + 2\varepsilon_m} = f\frac{\varepsilon - \varepsilon_m}{\varepsilon + 2\varepsilon_m}, \tag{1}$$

where ε_m, the dielectric permittivity of the matrix, f, the volume fraction of the metal phase and ε, the permittivity of an individual particle. In the theoretical calculation the size-dependent dielectric permittivity of different metallic phases have been estimated from the following relation (Granqvist and Hunderi 1977)

$$\varepsilon_j(\omega) = \varepsilon_{expt}(\omega) - \varepsilon_{expt}^{Drude}(\omega) + \varepsilon_j^{Drude}(\omega), \tag{2}$$

where, ω is the angular frequency of the concerned radiation

$$\varepsilon_{expt}^{Drude}(\omega) = 1 - \omega_{pb}^2/\omega(\omega + i/\tau_b) \tag{3}$$

and

$$\varepsilon_j^{Drude}(\omega) = 1 - \omega_{pd_j}^2/\omega\left(\omega + \frac{1}{\tau_j}\right) \tag{4}$$

ω_{pb}, τ_b being the bulk plasma frequency and the mean electron life time respectively. ω_{pd_j} denotes the apparent plasma frequency of particle size d_j and τ_j is given by

$$\frac{1}{\tau_j} = \frac{1}{\tau_b} + 2V_{Fb/dj}, \tag{5}$$

where V_{Fb} is the bulk Fermi velocity of electrons. Details of analyses along the lines discussed as above have been reported earlier for the four metal glass composites referred to in figure 1 (Chatterjee and Chakravorty 1989).

Quantum size effects in semiconductor nanocrystals like CdS, CdSe, CuBr, CuCl etc. dispersed in a glass matrix have been reported (Ekimov *et al* 1985; Warnock and Awschalom 1985). The optical absorption edge as measured at liquid helium temperature is found to be blue shifted as the crystallite size becomes smaller. Some of these materials have evoked considerable interest because of their possible nonlinear optical behaviour (Hanamma 1987).

3.2 *Electrical*

A wide range of resistivity can be induced in a glass metal nanocomposite by controlling the metal particle size and the inter-particle separation. Even when the metal phase percolates through the matrix resistivity values show a wide variation depending on the metal particle diameter.

Figure 2 shows the variation of resistivity as a function of temperature in the case of nanocomposites involving nickel, iron and copper respectively (Chatterjee and Chakravorty 1990). It is evident from this figure that resistivities varying over four orders of magnitude can be induced in the glass matrix by changing the metal phase and/or its diameter. In this figure particle sizes can be seen to have values in the range 4

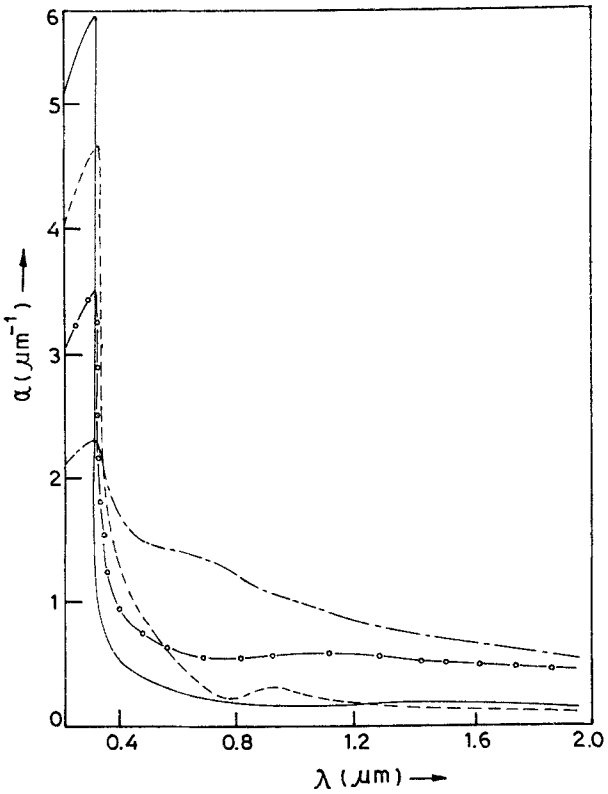

Figure 1. Optical absorption for various glass metal nanocomposites with different particle diameters d (Chatterjee and Chakravorty 1989). ——$Ni/SiO_2 = 5{\cdot}0$ nm; -----$Fe/SiO_2 = 3{\cdot}7$ nm; -○-○-$Mn/SiO_2 = 4{\cdot}3$ nm; -·-·-$Co/SiO_2 = 3{\cdot}6$ nm.

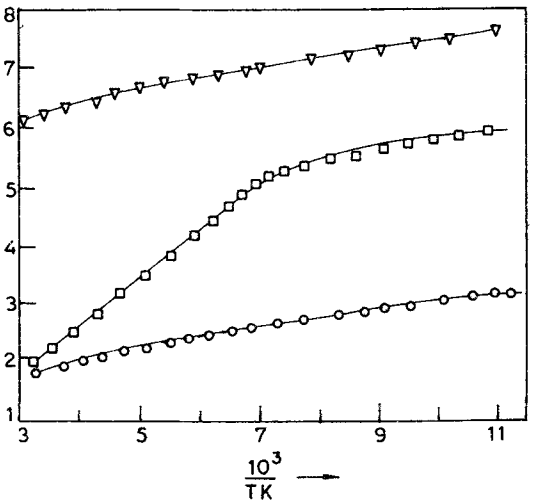

Figure 2. Resistivity as a function of temperature for different sol–gel derived glass metal nanocomposites (Chatterjee and Chakravorty 1990). ○Ni/SiO_2 $d = 10{\cdot}5$ nm; □Fe/SiO_2 $d = 3{\cdot}9$ nm; ▽Cu/SiO_2 $d = 4{\cdot}9$ nm.

to 10 nm. These nanocomposites have been prepared by the sol gel route as described in the previous section. It appears from these results that the resistivity is controlled by two activated mechanisms. The activation energy in the temperature range 150 to 300 K has values in the range 0·10 to 0·34 eV depending on the metallic species and the heat treatment schedule to which the precursor gel has been subjected. This has been explained as arising due to the localized states present within the band gap of the amorphous phase. These states are formed by the distributed metal atoms within the silica matrix. A hopping mechanism between these states contributes to the conductivity variation in this temperature range (Moyo and Leaver 1980).

The activation energy in the temperature range 90 to 150 K has values of the order of 0·01 to 0·10 eV. This has been ascribed to an electron tunnelling mechanism between the metallic islands (Neugebauer and Webb 1962). According to this model the electrical conductivity is given by (Adkins 1982)

$$\sigma = \sigma_0 \exp[-(2\alpha s + E/kT)] \tag{6}$$

where α is the tunnelling exponent for the electron wave function, s the inter-grain separation, E the activation energy for transport by electron tunnelling, k the Boltzmann constant and T the temperature.

The tunnelling exponent α has been shown to be given by (Abeles *et al* 1975)

$$\alpha = (2m\phi/\hbar^2)^{1/2}, \tag{7}$$

where m is the electronic mass, h the Planck's constant and ϕ the effective barrier height which is taken to be equal to the difference between the work function of the metal and the electron affinity of SiO_2.

The expression for activation energy E is as follows (Tick and Fehlner 1972)

$$E = \left(\frac{e^2}{4\pi\varepsilon_m}\right)\left[\frac{1}{r} - \frac{1}{(r+s)}\right] \tag{8}$$

where e is the electronic charge, r the radius of the metal particle and ε_m the dielectric permittivity of the matrix phase.

It is evident from (6), (7) and (8) that the electrical conductivity of glass metal nanocomposites can in principle be changed over a wide range by varying the particle size, inter-particle separation and the metallic species. The data in figure 2 illustrate this point. The details of analyses of the experimental results have been discussed earlier (Chatterjee and Chakravorty 1990).

Figure 3 shows the resistivity variation as a function of temperature for sol–gel derived iron silica glass nanocomposite in which the metallic phase has a percolation configuration. The data for three different metal particle diameters have been shown. It is seen that by reducing the metal particle size the room temperature resistivity can be changed by a factor of 30. Similar data have been observed in the case of copper silica nanocomposites also with particle size varying from 5·9 to 12·6 nm (Chatterjee and Chakravorty 1992). In figure 4 is shown the variation of surface resistivity as a function of temperature for silver particles grown within a glass-ceramic by ion exchange and reduction technique and having diameters varying from 4·3 nm to 11·0 nm. Here also we find a wide range of resistivity induced in the precursor solid by a change of metal particle size. In order to study the effect of particle size on the physical mechanism

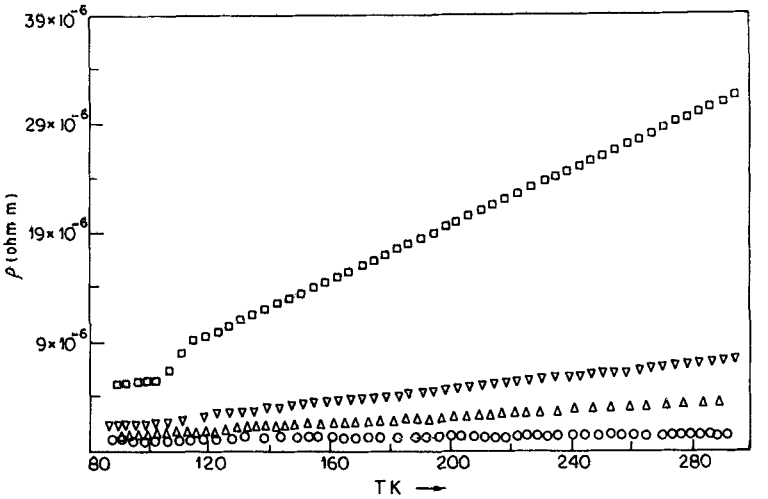

Figure 3. Resistivity as a function of temperature for sol–gel derived Fe/SiO_2 nanocomposites in percolation configuration (Chatterjee and Chakravorty 1992). □ 3·4 nm; ▽ 5·6 nm; △ 8·3 nm; ○ 9·3 nm.

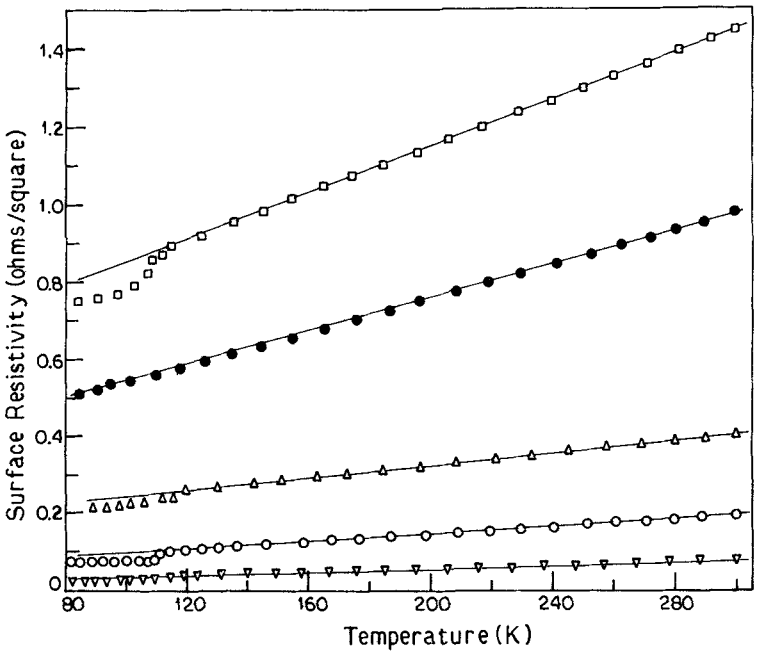

Figure 4. Surface resistivity vs temperature for Ag/SiO_2 nanocomposites prepared by ion exchange/reduction route (Roy and Chakravorty 1990). □ 4·3 nm; ● 4·8 nm; △ 6·6 nm; ○ 8·3 nm; ▽ 11·0 nm.

causing electrical conduction in these nanocomposites, Ziman's (1960) expression for a bulk metal can be used viz

$$\rho_L = \frac{C}{\theta_D}\left(\frac{T}{\theta_D}\right)^5 \int_0^{\theta_D/T} z^5 \, dz/[(e^z - 1)(1 - e^{-z})] \tag{9}$$

where ρ_L is the resistivity due to lattice vibrations, θ_D the Debye temperature, T the

Table 1. θ_D values for different nanocomposites.

System	Particle diameter (nm)	θ_D (K)	Reference
Aluminium	15	200	Fujita *et al* (1976)
	20	291	—
Silver	10	165	—
	30	188	—
Fe/SiO_2	9·5	408	Chatterjee and Chakravorty (1992)
	8·3	390	—
	5·6	361	—
	3·4	346	—
Cu/SiO_2	12·6	307	—
	10·5	288	—
	7·8	261	—
	5·9	243	—
Ag/SiO_2	11·0	192	Roy and Chakravorty (1990)
	8·3	163	—
	7·2	155	—
	6·6	154	—
	5·5	126	—
	4·8	105	—
	4·6	103	—
	4·3	98	—

temperature and C a constant. Several authors have used the above equation to analyse electrical resistivity behaviour of systems consisting of ultrafine metallic particles (Fujita *et al* 1976; Edwards 1986; Roy and Chakravorty 1990). Electrical resistivity data in several systems have been fitted to (9) treating θ_D as a floating parameter. The value of effective Debye temperature has been reported to decrease as the metal particle size is reduced. Table 1 summarizes the data obtained in the case of Fe/SiO_2, Cu/SiO_2 and Ag/SiO_2 systems respectively. Data from small metal particles of aluminium and silver in thin films are also given in this table. Such a decrease in the value of θ_D is referred to as phonon-softening. This is believed to arise due to the modification of the phonon spectra of an ultra fine particle from that of the bulk metal in two ways: (a) a finite size of the particle leads to a low-frequency cut-off and (b) the vibrational potential of the surface atoms becomes weaker causing a general lowering of phonon frequencies. Another effect observed in the small particle conductivity behaviour as shown in figures 3 and 4 is the change of slope in the resistivity temperature plot at around 120 K. This property has been explained on the basis of the presence of different regions in the metal aggregates which have two different fractal dimensions (Roy and Chakravorty 1990).

3.3 *Magnetic*

The most useful magnetic property observed in the case of small ferromagnetic metal particles is the increase in the value of their coercivity. The coercivity at a temperature

T for a single domain particle is given by (Yiping *et al* 1990)

$$H_c = \frac{2K}{M_s}\left[1 - \left(\frac{T}{T_B}\right)^{1/2}\right] \tag{10}$$

where K is the anisotropy energy density constant, M_s the saturation magnetization and T_B the blocking temperature. H_c values of single domain particles are very high below T_B. Above this temperature the particles exhibit superparamagnetism. Coercivity value of the order of 2500 Oe at 2 K has been reported in the case of ultrafine particles of iron with sizes in the range 1·7 to 7 nm distributed in a silica matrix – the composites being synthesized by r.f. magnetron sputtering (Xiao and Chien 1987). Nanocrystalline Fe, Co and Ni respectively prepared by the gas evaporation technique have shown coercivity values of 1000, 1500 and 450 Oe the particle sizes being 21, 20 and 31 nm respectively (Gong *et al* 1991). Mössbauer spectroscopy has been used to observe super paramagnetic relaxation in nanocrystalline iron and iron-chromium alloy in a silica glass matrix (Chatterjee *et al* 1990).

There have been a number of studies—both theoretical and experimental—regarding the electron spin resonance (ESR) spectra in ultrafine metallic particles (Kawabata 1970; Saiki *et al* 1972; Buttet *et al* 1982). A size dependent g shift has been predicted theoretically though the nature of variation differs for different authors. The most recent ESR measurements on nanocrystalline Li, Ag and Au having particle sizes in the range 2 to 8 nm show no ESR signal due to quantum size effect (Sako 1990).

4. Summary

Nanocomposites comprising nanocrystalline metals dispersed in a host matrix can be synthesized by various physical and chemical methods. Some of the latter like sol–gel and ion exchange followed by reduction of suitable glass-ceramics have been found to be convenient for studying the effect of small particle size of different metallic species on their electrical, optical and magnetic behaviour. By controlling the volume fraction of the metal phase and the particle size of the latter electrical conductivity values over a wide range can be generated. In the non-percolative configuration the electrical conduction arises due to an electron tunnelling mechanism. The metallic conduction on the other hand is characterized by a gradual lowering of the effective Debye temperature as the particle size is reduced. Nanocrystalline ferromagnetic metals dispersed in a non-magnetic matrix show high values of magnetic coercivity.

Acknowledgement

The author thanks the Department of Science and Technology for supporting his research on nanocomposites.

References

Abeles B, Sheng P, Coutts M D and Arie Y 1975 *Adv. Phys.* **24** 407

Adkins C J 1982 *J. Phys. C: Solid State Phys.* **15** 7143

Andres R P, Averback R S, Brown W L, Brus L E, Goddard III W A, Kalador A, Louie S G, Moscovits M, Peercy P S, Riley S J, Siegel R W, Spaepen F and Wang Y 1989 *J. Mater. Res.* **4** 704

Armistead W H and Stookey S D 1965 US Pat. No. 3108860
Birringer R, Gleiter H, Klein H P and Marquardt P 1984 *Phys. Lett.* **A102** 365
Buttet J, Car R and Myles C W 1982 *Phys. Rev.* **26** 2414
Chakravorty D 1992 in *New materials* (ed.) S K Joshi, C N R Rao, T Tsuruta and S Nagakura (New Delhi: Narosa Publishing House) pp 170
Chakravorty D and Giri Anit K 1992 in *Chemistry of advanced materials* (ed.) C N R Rao (Oxford: IUPAC/Blackwell) (to be published)
Chatterjee A and Chakravorty D 1989 *J. Phys. D: Appl. Phys.* **22** 1386
Chatterjee A and Chakravorty D 1990 *J. Phys.* **D23** 1097
Chatterjee A, Das D, Chakravorty D and Choudhury K 1990 *Appl. Phys. Lett.* **57** 1360
Chatterjee A and Chakravorty D 1992 *J. Mater. Sci.* (in print)
Childress J R, Chien C L and Nathan M 1990 *Appl. Phys. Lett.* **56** 95
Doremus R H 1965 *J. Chem. Phys.* **42** 414
Edwards P P 1986 in *Advances in solid state chemistry* (ed.) C N R Rao (New Delhi: Indian National Science Academy) pp 265
Ekimov A I, Efros A L and Onuschenko A A 1985 *Solid State Commun.* **56** 921
Fujita T, Ohshima K and Kouroishi T 1976 *J. Phys. Soc. Jpn.* **40** 90
Gong W, Li H, Zhao Z and Chen J 1991 *J. Appl. Phys.* **69** 5119
Granqvist C G and Buhrman R A 1976 *J. Appl. Phys.* **47** 2200
Granqvist C G and Hunderi O 1977 *Phys. Rev.* **B16** 3513
Hanamma E 1987 *Solid State Commun.* **62** 465
Hayashi R, Yamamoto M, Tsunetomo K, Kohno K, Osaka Y and Nasu H 1990 *Jpn. J. Appl. Phys.* **29** 756
Kawabata A 1970 *J. Phys. Soc. Jpn* **29** 902
Kreibig U 1974 *J. Phys.* **F4** 999
Maxwell-Garnett J C 1904 *Philos. Trans. R. Soc. (London)* **203** 385
Moyo N D and Leaver K D 1980 *J. Phys.* **D13** 1511
Neugebauer C A and Webb M B 1962 *J. Appl. Phys.* **33** 74
Roy R A and Roy R 1984 *Mater. Res. Bull.* **19** 169
Roy B and Chakravorty D 1990 *J. Phys.: Condens. Matter* **2** 9323
Saiki K, Fujita T, Shimizu Y, Sako S and Wada N 1972 *J. Phys. Soc. Jpn* **32** 447
Sako S 1990 *J. Phys. Soc. Jpn* **59** 1366
Stookey S D, Beall G H and Pierson J E 1978 *J. Appl. Phys.* **49** 5114
Tick P A and Fehlner F P 1972 *J. Appl. Phys.* **43** 362
Warnock J and Awschalom D D 1985 *Phys. Rev.* **B32** 5529
Xiao G and Chien C L 1987 *Appl. Phys. Lett.* **51** 1280
Yiping L, Hdjinanayis G C, Sorensen C M and Klabunde K J 1990 *J. Appl. Phys.* **67** 4502
Ziman J M 1960 *Electrons and phonons* (Oxford: Clarendon) p. 364